The Journal of Physical Chemistry

 VOLUME 97, NUMBER 13, APRIL 1, 1993

LETTERS

Time Dependence of the Photodissociation of $Sr^+(NH_3)_2$

C. A. Schmuttenmaer, J. Qian, S. G. Donnelly, M. J. DeLuca,† D. F. Varley, L. A. DeLouise,‡ R. J. D. Miller, and J. M. Farrar*

Center for Photoinduced Charge Transfer and Department of Chemistry, University of Rochester, Rochester, New York 14627

Received: November 2, 1992; In Final Form: January 14, 1993

We present measurements of the time dependence of the $Sr^+(NH_3)_2 \rightarrow Sr^+(NH_3) + NH_3$ photodissociation process. Equal intensity pump and probe laser pulses obtained from a three-stage, synchronously pumped, picosecond dye laser amplifier are used to photodissociate mass-selected $Sr^+(NH_3)_2$ parent ions. The $Sr^+(NH_3)$ daughter and Sr^+ granddaughter ions are detected with a reflectron mass spectrometer. Photodissociation is dominated by a process that has a 6.7 ± 0.7 ns time constant.

The field of time domain measurements of reaction dynamics has been extremely active for over two decades.[1] Recent advances in subpicosecond pulsed laser techniques have allowed the direct study of the dynamical properties of molecular systems on increasingly shorter time scales.[2] In favorable cases involving relatively simple systems, such as ICN, NaI, I_2, and Ne–I_2, reaction probabilities have been measured in real time.[3-6] Time-resolved pump–probe studies have also been carried out with more complicated systems. The time required for absorption recovery from geminate recombination after photodissociation of the I_2^- ion solvated by CO_2 molecules has been measured in mass-selected $I_2^-(CO_2)_n$ clusters with $n = 9$ and 16,[7,8] and proton transfer in solvated phenol clusters has been investigated by monitoring branching ratios upon time-resolved two-photon ionization.[9] More recently, Gerber and collaborators[10] have made real-time measurements of the ejection of Na_2 and Na_3 photofragments from ionized sodium clusters on the femtosecond time scale. These latter two experiments employ mass-resolved product detection without initial parent mass selection.

Because condensed-phase processes involve numerous many-body interactions, dynamical information is often highly collisionally averaged. The study of dynamical processes in size-selected clusters affords an opportunity to separate intrinsic collision dynamics from the perturbations of solvent molecules, and this realization has led to several recent time-dependent studies of chemical reactions and photodissociation in such species.[3,8-11] In this Letter, we demonstrate initial results from an experiment designed to probe the dynamics of solvent motion in mass-selected gas-phase cluster ions. Recent work from our laboratory on the absorption spectroscopy of mass-selected $Sr^+(NH_3)_n$ clusters for $n = 1$–6 has shown a strong size-dependent red shift that signals the onset of spontaneous ionization of Sr^+ and stabilization of the electron by several solvent molecules.[12,13] The analogy between this process in clusters and the bulk phenomenon of electron solvation suggests that time domain measurements of photodissociation processes in these clusters will provide insight into the nature of photoinduced charge transfer and concomitant solvent motion in finite aggregates. As an initial step in probing the time dependences of such solvent reorganization processes, we report a study of the photodissociation of $Sr^+(NH_3)_2$, both as a measure of solvent dynamics and as a demonstration that time-resolved, gas-phase, mass-selected studies are experimentally accessible in solvated metal ion systems. In addition, the experiment demonstrates that the dissociation lifetime is on the nanosecond time scale, rather than the picosecond time scale expected for direct and predissociative processes in small molecules.[3,5,14,15] Among the extant studies of time-resolved processes in clusters, only the present study and the pioneering work of Lineberger and collaborators[7,8] have been carried out with initial mass selection of the parent ions. This point is critical in identifying unambiguously the carrier of the spectrum, as well as in determining the parentage of all photofragments.

† Present address: Eastman Kodak Co., Rochester, NY 14650-2132.
‡ Xerox Corporation, Webster, NY 14580.

0022-3654/93/2097-3077$04.00/0

In the work presented here, in which we carry out a pump and probe study of $Sr^+(NH_3)_2$ photodissociation, the pump photon excites the cluster from the $^2A_{1g}$ ground state to the ^2E_u excited electronic state.[16] This transition correlates to the atomic $^2P \leftarrow {}^2S$ transition in the bare Sr^+ ion. The system undergoes a transition from the bound excited state to the ground-state surface above its dissociation limit, resulting in the loss of one NH_3 ligand. The $Sr^+(NH_3)$ daughter ion can then absorb a photon from the probe pulse leading to its dissociation into Sr^+ and NH_3. Thus, the intensity of bare Sr^+ ion signal as a function of pump–probe delay will describe the growth of the $Sr^+(NH_3)$ population after initial excitation of $Sr^+(NH_3)_2$ with the pump pulse. The $Sr^+(NH_3)_2 \rightarrow Sr^+(NH_3) \rightarrow Sr^+$ system is unique among the ammoniated Sr^+ clusters in that the absorptions of $Sr^+(NH_3)_2$ and $Sr^+(NH_3)$ both peak at 580 nm,[17] thereby allowing the dynamics to be measured in a one-color, two-pulse experiment.

The experimental apparatus is similar to that described by Ray et al.[7] and can be divided into three parts. Cluster ions are produced by a standard laser vaporization source in which 532-nm radiation strikes a disk of Sr in synchronization with the injection of a mixture of NH_3 and He from a pulsed valve. The ions are mass-selected by a Wiley-McLaren TOF mass spectrometer and undergo photolysis with a picosecond laser system, consisting of a picosecond seed laser which is then further amplified. The seed laser is a synchronously pumped, cavity dumped picosecond dye laser pumped by the second harmonic of a mode-locked Nd^{3+}:YAG laser yielding approximately 5–20-nJ, 1–10-ps pulses at 580 nm when using Rhodamine 590 dye and DODCI saturable absorber. Pulses selected from the 3.8-MHz cavity dumped pulse train are then amplified by a three-stage synchronously pumped dye laser amplifier. The pump pulses for the amplifier are provided by doubling the output of a regenerative amplifier seeded by the residual IR after doubling the mode-locked YAG. The output of the dye amplifier is typically 700 μJ/pulse at 30 Hz for 1–2-ps pulses and 1.2 mJ/pulse for 8–10-ps pulses. Approximately 8% of the beam is directed into a photodiode in order to monitor both the laser power and shot-to-shot fluctuations; these measurements show that the power does not vary by more than 10% during a given session of data collection.

We obtain dynamical information regarding the photodissociation of $Sr^+(NH_3)_2$ using 8–10 ps long pump and probe pulses and pump–probe delays of up to 16 ns. A mirror was placed from 15 to 240 cm from the chamber center line to provide the appropriate delay as well as to double pass the laser beam and improve the signal-to-noise ratio. The temporal resolution due to counterpropagating pump and probe pulses across a 1-cm-diameter ion beam is about 45 ps, which is quite adequate for following the nanosecond dynamics.

The data are acquired by recording the mass spectrum containing the residual parent $[Sr^+(NH_3)_2]$, daughter $[Sr^+(NH_3)]$, and granddaughter $[Sr^+]$ species with a 100-MHz transient digitizer and averaging together 200 shots to obtain an acceptable signal-to-noise ratio. Each peak is numerically integrated and then normalized to the sum of residual parent, daughter, and granddaughter signal to account for shot-to-shot variations in the cluster source. The amount of photodissociation product as a function of pump–probe delay is a measure of the dynamics of $Sr^+(NH_3)_2$ dissociation. Figure 1 presents the mass spectrum of $Sr^+(NH_3)_2$ and its photofragments with the pump and probe laser off and on, taken at a laser pulse energy of 400 μJ. When the laser is off (top panel) only the mass representing the $Sr^+(NH_3)_2$ parent ion is present, and the three main isotopes of Sr (82.6% ^{88}Sr, 7.0% ^{87}Sr, 9.9% ^{86}Sr) are easily distinguished. The lower panel of Figure 1 is obtained when the laser is timed to photodissociate $^{88}Sr^+(NH_3)_2$, and the pump–probe delay is 10 ns. Typically, 3–8 such integrations are done for a given pump–probe delay to obtain the average and standard deviation for the

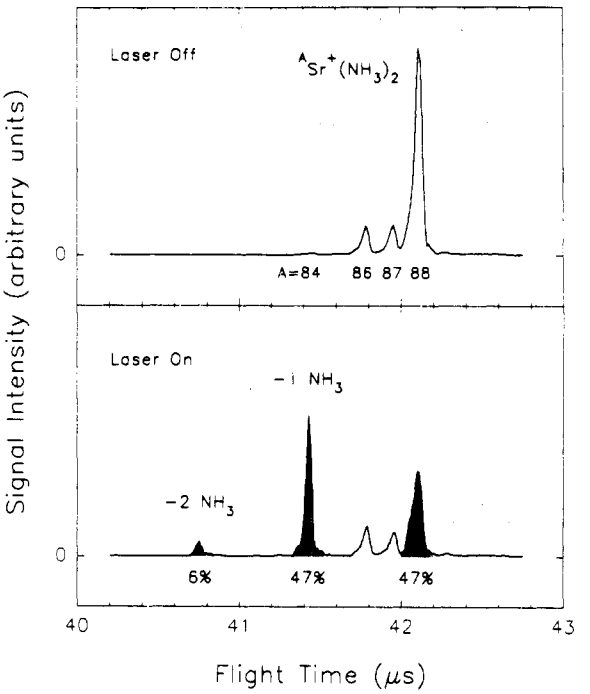

Figure 1. TOF mass spectra of $Sr^+(NH_3)_2$ and photoproducts. In the upper panel, the dissociation laser is off and only the parent $Sr^+(NH_3)_2$ ion is observed. The three peaks represent the main isotopes of Sr (82.6% ^{88}Sr, 7.0% ^{87}Sr, 9.9% ^{86}Sr)[12] and are easily distinguished. In the lower panel, the pump and probe pulses are separated by 10 ns. The pump pulse is timed to dissociate the $^{88}Sr^+(NH_3)_2$ parent. Nearly equal intensities of parent and daughter ion signals are consistent with the saturation of the first transition in the sequential dissociation process.

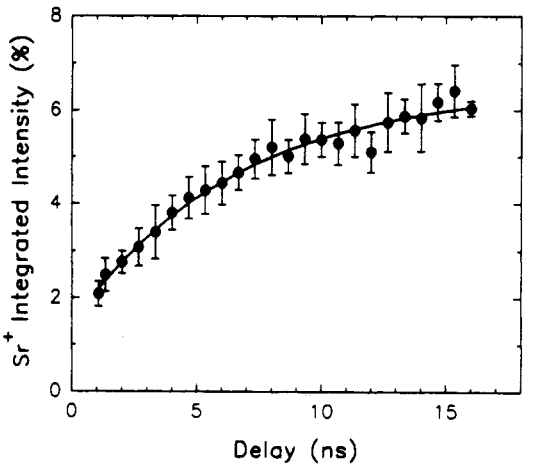

Figure 2. Granddaughter Sr^+ ion intensity as a function of pump–probe delay. The experimental measurements and uncertainties are indicated with filled circles and error bars, respectively. The solid line through the data is an exponential growth function with a time constant of 6.7 ns.

granddaughter, daughter, and residual parent signals. We collected mass spectra for a range of pump and probe delay times up to 16 ns. The data we obtain are in the form of integrated Sr^+ intensity normalized to the parent ion intensity.

Figure 2 shows the experimental data for the appearance of Sr^+ granddaughter ions as a function of the delay time between the pump and probe pulses. The data are shown with a fit to an exponential growth function having a time constant of 6.7 ± 0.7 ns. At a pulse energy of 400 μJ for each of the pump and probe beams, up to 6% of the parent clusters absorb both a pump and probe photon. The exponential rise at long delay times provides qualitative confirmation of the sequential ligand loss mechanism.

Experiments that determine how photofragment intensities depend on laser fluence reveal critical information about the kinetics of photon absorption and the subsequent loss of two solvent

molecules. Independent work from this laboratory[17,18] on the single-photon absorption cross sections of $Sr^+(NH_3)_2$ and $Sr^+(NH_3)$ shows that the loss of the first ligand from $Sr^+(NH_3)_2$ takes place with a cross section over an order of magnitude larger than for the loss of the second ligand. The mass spectrum in the lower panel of Figure 1 is consistent with these relative cross sections in that essentially complete saturation of the first transition is observed as evidenced by the equal parent and daughter intensities and the significantly smaller granddaughter intensity. Studies of Sr^+ production at delays in the nanosecond regime performed with picosecond width pulses show a linear dependence on fluence, also consistent with the sequential mechanism and saturation of the first transition implicit in the data of Figure 2.

The dissociation time of 6.7 ns is comparable to pulse widths from conventional nanosecond lasers: under such conditions, the fluence dependences of $Sr^+(NH_3)_2$ depletion and the appearance of $Sr^+(NH_3)$ and Sr^+ photoproducts also yield insight into the kinetics of the dissociation process. We have performed such a series of measurements[19] over a range of fluences up to 60 mJ cm^{-2}. The data we obtain are in good agreement with a sequential mechanism

$$Sr^+(NH_3)_2 \xrightarrow{\sigma_{21}} Sr^+(NH_3) \xrightarrow{\sigma_{10}} Sr^+$$

in which the fluence dependences of each species are given below. In the following expressions, the brackets denote ion fluxes as a function of fluence Φ, M denotes Sr^+, L denotes the ligand NH_3, and the ligand loss cross sections are as defined above:

$$[ML_2]_\Phi = [ML_2]_0 \exp(-\sigma_{21}\Phi)$$

$$[ML]_\Phi = [ML_2]_0\{\sigma_{21}/(\sigma_{10} - \sigma_{21})\}\{\exp(-\sigma_{21}\Phi) - \exp(-\sigma_{10}\Phi)\}$$

$$[M]_\Phi = [ML_2]_0 - [ML_2]_\Phi - [ML]_\Phi$$

The experimental fluence data can be fitted to cross sections σ_{21} and σ_{10} in excellent agreement with those determined in independent measurements on mass-selected clusters. These measurements provide additional support for the sequential nature of the dissociation process.

The exponential growth function in Figure 2 has a finite intercept at zero delay, corresponding to 1.4% of the initial parent ion intensity or nearly 25% of the asymptotic Sr^+ signal. While the long-time behavior of the system is the dominant decay channel, this zero delay signal indicates a second channel producing Sr^+ that is fast compared to the laser pulse width. This zero delay signal results from either the sequential absorption of two photons from the same laser pulse or the loss of both ligands upon absorption of one photon. We tested the first possibility by performing careful single-pulse measurements with 1–2-ps laser pulses as a function of fluence, from 2 mJ cm^{-2} down to the detection limit for Sr^+, and found a linear dependence. This is the result that we would expect from a sequential process if the first transition is saturated, as we noted earlier. The second possibility is unlikely since parent clusters with significant amounts of internal energy would be required and should yield a metastable decay signal on the instrument transit time scale. We observed no such metastable signal, consistent with the fact that clusters produced in the supersonic expansion have vibrational and rotational temperatures of no more than 100 K.[20] We also performed measurements at short times by scanning ±10 ps relative to zero delay using copropagating pump and probe pulses in hopes of seeing indications of dissociation processes that are faster than the laser pulse width. The shortest time scales that can be deconvoluted from the laser pulse width are $^1/_3$ to $^1/_4$ as long as the fwhm of the pulse width. Several attempts were made to see a feature at $t = 0$ when using 1–2-ps pulse widths, but none were successful, implying the existence of a secondary process that is faster than 1 ps.

The time constant of the exponential growth function is a measure of the rate of the dominant dissociation process. We have interpreted the dissociation dynamics of these complexes are predissociative in character, a point support by ab initio calculations showing that the excited states are bound.[16] The 6.7-ns time constant reflects the time required for the $Sr^+(NH_3)_2$ cluster ion to cross back from the initially accessed bound excited state to vibrational levels of the ground state that lie above the dissociation barrier, as well as the time required for the system to evolve along the dissociation coordinate in the ground state. On this time scale, fluorescence could also provide a mechanism for returning to the ground-state surface, but direct detection of the fluorescent photons was not possible in our experimental geometry. Although 6.7 ns is surprisingly long in comparison with the picosecond lifetimes characteristic of small molecule photodissociation, a statistical RRKM calculation[21] of the decay rate for $Sr^+(NH_3)_2$ yields results in reasonable agreement with our measured value. However, we are reluctant to describe the decay as statistical, since such models would predict an increase in lifetime with increasing cluster size: preliminary results from our laboratory[22] suggest instead that dissociation lifetimes decrease by at least 1 order of magnitude as additional solvent molecules are added to these clusters.

The photodissociation process we observe appears to channel electronic energy into vibrational excitation on the ground potential energy surface. A number of studies on the nature of electronic to vibrational energy transfer between excited alkali-metal atoms and molecular collision partners[23-27] suggest that internal motions in the collision partner are critical in the quenching process. The bond-stretch attraction model described by Hertel[28] focuses on the role of vibrational motion in the collision partner and the fact that such motions result in crossings between electronic ground and excited potential energy surfaces. For example, ab initio calculations on $Na^* + N_2$[29] and H_2[30] show that surface crossings between electronically excited states and the ground state only occur when the N–N or H–H bonds are distorted from their equilibrium values.

The role of collisional charge transfer in E–V energy exchange has been discussed recently[31] in the context of quenching $Ba(^1P_1)$ by O_2, N_2, NO, and H_2. That study underscored the important role played by electron transfer, particularly in systems where the collision partner has a positive electron affinity and the anion has favorable Franck–Condon factors connecting its vibrationally excited levels to vibrational states of the neutral molecule. Even in cases where a stable anion does not exist, however, ab initio calculations[30] suggest that significant transfer of electron density from the metal to the collision partner occurs near potential surface crossings, where the molecule is distorted from its equilibrium geometry. The similarities in the electronic structure of these collisional systems to those of the clusters studied here suggest a clear dynamical analogy as well. This analogy is strengthened by the fact that, in other experimental work from our laboratory,[13] we have shown that $\langle r^2 \rangle$ for the ground-state valence electron radial probability distribution in $Sr^+(NH_3)_n$ for $n = 1$–6 expands by an order of magnitude, consistent with Rydberg state formation and electron delocalization into the solvent. Path integral Monte Carlo structural calculations on these systems by Martyna and Klein[32] are also consistent with this interpretation. The possible role of charge transfer in describing the size-dependent spectra of these clusters suggests that time-dependent studies hold promise for elucidating the role of solvent motion and charge rearrangement in the photodissociation dynamics of these systems. The present work on $Sr^+(NH_3)_2$ represents the first in a series of studies in our laboratory that will address these issues.

The work presented here demonstrates the feasibility of studying solvent dynamics in mass-selected gas-phase solvated metal ions.

The initial results show that the $Sr^+(NH_3)_2$ photodissociation process takes on the order of 7 ns. Future work will include extending these studies to larger $Sr^+(NH_3)_n$ clusters, as well as to different metal ions and/or different ligands. The goal of these studies is to enhance our understanding of the structural and dynamical features of the solvation process in condensed phases.

Acknowledgment. We gratefully acknowledge support of this research through the Center for Photoinduced Charge Transfer. J.M.F. also acknowledges support through National Science Foundation Grant CHE-9122170 as well as from the donors of the Petroleum Research Fund, administered by the American Chemical Society. Helpful discussions with Dr. Thomas E. Orlowski are also gratefully acknowledged.

References and Notes

(1) Khundkar, L. R.; Zewail, A. H. *Annu. Rev. Phys. Chem.* **1990**, *41*, 15.
(2) Fleming, G. R. *Chemical Applications of Ultrafast Spectroscopy*; Oxford University Press: New York, 1986.
(3) Willberg, D. M.; Gutmann, M.; Breen, J. J.; Zewail, A. H. *J. Chem. Phys.* **1992**, *96*, 198.
(4) Gruebele, M.; Roberts, G.; Dantus, M.; Bowman, R. M.; Zewail, A. H. *Chem. Phys. Lett.* **1990**, *166*, 459.
(5) Rosker, M. J.; Rose, T. S.; Zewail, A. H. *Chem. Phys. Lett.* **1988**, *146*, 175.
(6) Gruebele, M.; Zewail, A. H. *Ber. Bunsen-Ges. Phys. Chem.* **1990**, *94*, 1210.
(7) Ray, D.; Levinger, N. E.; Papanikolas, J. M.; Lineberger, W. C. *J. Chem. Phys.* **1989**, *91*, 6533.
(8) Papanikolas, J. M.; Gord, J. R.; Levinger, N. E.; Ray, D.; Vorsa, V.; Lineberger, W. C. *J. Phys. Chem.* **1991**, *95*, 8028.
(9) Syage, J. A.; Steadman, J. *J. Chem. Phys.* **1991**, *95*, 2497. Steadman, J.; Syage, J. *J. Am. Chem. Soc.* **1991**, *113*, 6786.
(10) Baumert, T.; Röttgermann, C.; Rothenfusser, C.; Thalweiser, R.; Weiss, V.; Gerber, G. *Phys. Rev. Lett.* **1992**, *69*, 1512.
(11) Li, S.; Bernstein, E. R. *J. Chem. Phys.* **1992**, *97*, 792.
(12) Shen, M. H.; Farrar, J. M. *J. Phys. Chem.* **1989**, *93*, 4386.
(13) Donnelly, S. G.; Farrar, J. M. *J. Chem. Phys.*, submitted for publication.
(14) Dzvonik, M.; Yang, S.; Bersohn, R. *J. Chem. Phys.* **1974**, *61*, 4408.
(15) Yang, S.; Bersohn, R. *J. Chem. Phys.* **1976**, *61*, 4400.
(16) Bauschlicher, C. W., Jr.; Sodupe, M.; Partridge, H. W. *J. Chem. Phys.* **1992**, *96*, 4453.
(17) Shen, M. H.; Farrar, J. M. *J. Chem. Phys.* **1991**, *94*, 3322.
(18) Donnelly, S. G.; Farrar, J. M. *J. Chem. Phys.*, in press.
(19) Shen, M. H. Ph.D. Dissertation, University of Rochester, 1990.
(20) Donnelly, S. G.; Farrar, J. M. *Chem. Phys. Lett.*, to be published.
(21) Marcus, R. A. *J. Chem. Phys.* **1952**, *20*, 352.
(22) Schmuttenmaer, C. A.; Qian, J.; Donnelly, S. G.; Farrar, J. M. Unpublished work.
(23) Hertel, I. V.; Hoffmann, H.; Rost, K. A. *Phys. Rev. Lett.* **1976**, *36*, 861.
(24) Hertel, I. V.; Hoffmann, H.; Rost, K. A. *Chem. Phys. Lett.* **1977**, *47*, 163.
(25) Hertel, I. V.; Hoffmann, H.; Rost, K. A. *J. Chem. Phys.* **1979**, *71*, 674.
(26) Hertel, I. V.; Reiland, W. *J. Chem. Phys.* **1981**, *74*, 6757.
(27) Silver, J. A.; Blais, N. C.; Kwei, G. H. *J. Chem. Phys.* **1979**, *71*, 3413.
(28) Hertel, I. V. *Adv. Chem. Phys.* **1982**, *50*, 475.
(29) Habitz, P. *Chem. Phys.* **1980**, *54*, 131.
(30) Botschwina, P.; Meyer, W.; Hertel, I. V.; Reiland, W. *J. Chem. Phys.* **1981**, *75*, 5438.
(31) Suits, A. G.; De Pujo, P.; Sublemontier, O.; Visticot, J.-P.; Berlande, J.; Currelier, J.; Gustavsson, T.; Mestdagh, J.-M.; Meynadier, P.; Lee, Y. T. *J. Chem. Phys.* **1992**, *97*, 4094.
(32) Martyna, G. J.; Klein, M. L. *J. Phys. Chem.* **1991**, *95*, 515.